Oxidative Addition of Alkyl Halides to Rhodium(I) and Iridium(I) Dicarbonyl Diiodides: Key Reactions in the Catalytic Carbonylation of Alcohols

Paul R. Ellis, Jean M. Pearson, Anthony Haynes, Harry Adams, Neil A. Bailey, and Peter M. Maitlis*

Department of Chemistry, The University of Sheffield, Sheffield S3 7HF, England

Received March 23, 1994[⊗]

Alkyl iodides (RI) react with $[Rh(CO)_2I_2]^-$ to give *acyl* species $[Rh(CO)(COR)I_3]^-$ (R = Et, ^{n}Pr, ^{i}Pr) and with $[Ir(CO)_2]_2]^-$ to give *alkyl* complexes $[RIr(CO)_2I_2]^-$ (R = Et, ^{n}Pr, ^{i}Pr, ^{n}Bu, *n*-C_5H_{11}, *n*-C_6H_{13}). The reactions are analogous to the known reactions of MeI with $[Rh(CO)_2I_2]^-$ and $[Ir(CO)_2I_2]^-$. The products are characterized spectroscopically and by an X-ray crystal structure determination for $Ph_4As[(n\text{-}C_6H_{13})Ir(CO)_2I_3]$ which showed a *fac,cis* geometry for the anion. [Crystal structure data: monoclinic, a = 9.408(7) Å, b = 19.470(16) Å, c = 19.529(12) Å, β = 94.99(5)°, Z = 4, space group $P2_1/n$ (a nonstandard setting of $P2_1/c$ C_{2h}^5, No. 14); 2446 independent reflections (of 5197 measured) for which $|F|/\sigma(|F|) > 4.0$; R = 0.0966 (R_w = 0.0921, 238 parameters)]. Kinetic data for the reactions of $[Rh(CO)_2I_2]^-$ with EtI, ^{n}PrI, and ^{i}PrI and for $[Ir(CO)_2I_2]^-$ with MeI, EtI, and ^{n}PrI show that oxidative addition of RI to $[M(CO)_2I_2]^-$ is first-order in both reactants. For M = Rh, reactions showed clean second-order kinetics below 80 °C, though some decomposition occurred at higher temperatures. For M = Ir, clean second-order kinetics were observed with MeI, but reactions with EtI and ^{n}PrI showed a more complex kinetic behavior. A competing radical pathway is suggested, which can be quenched by added duroquinone. Second-order rate constants, k_2, evaluated over the temperature ranges 70–80 °C (M = Rh) and 35–50 °C (M = Ir) gave the following activation parameters: (M = Rh) $\Delta H^{\ddagger}$/kJ mol^{-1} = 50(±1) (R = Me), 56(±10) (R = Et), 51(±10) (R = ^{n}Pr), 61(±15) (R = ^{i}Pr); $\Delta S^{\ddagger}$/J mol^{-1} K^{-1} = −165(±4) (R = Me), −195(±25) (R = Et), −215(±25) (R = ^{n}Pr), −180(±30) (R = ^{i}Pr); (M = Ir) $\Delta H^{\ddagger}$/kJ mol^{-1} = 54(±1) (R = Me), 66(±5) (R = Et), 66(±3) (R = ^{n}Pr); $\Delta S^{\ddagger}$/J mol^{-1} K^{-1} −113(±4) (R = Me), −123(±15) (R = Et), −132(±11) (R = ^{n}Pr). Comparisons are made between the reactions of methyl iodide and the higher alkyl iodides with both $[Rh(CO)_2I_2]^-$ (relative rates: Me, 1000, Et, 3; ^{n}Pr, 1.7) and $[Ir(CO)_2I_2]^-$ (relative rates: Me, 1000; Et, 2.3; ^{n}Pr, 0.75). The similarity to reactivity trends for organic nucleophiles suggests an S_N2 mechanism, but with a competing radical pathway for iridium. Relative rates for the two nucleophiles, k_{Ir}/k_{Rh} ca. 150 (R = Me), 220 (R = Et), and 140 (R = ^{n}Pr), are estimated. Alkyl isomerization (iso → n) is observed for both $[Rh(CO)(COPr)I_3]^-$ and $[PrIr(CO)_2I_3]^-$ and displacement of propene from $[Rh(CO)(COPr)I_3]^-$ by added ethene gives $[Rh(CO)(COEt)I_3]^-$ reversibly. A mechanism involving hydridoalkene intermediates is proposed. The data are consistent with the carbonylation of the higher alcohols (ROH) proceeding via rate determining oxidative addition of RI to $[Rh(CO)_2I_2]^-$, rather than by a route involving a rhodium hydride addition to an olefin derived from the ROH.

Introduction

Oxidative addition of methyl iodide to $[Rh(CO)_2I_2]^-$ (**1**) is the key organometallic step in the industrially important rhodium and iodide catalyzed carbonylation of methanol to acetic acid.[1] The mechanism of this reaction has been discussed in some detail in recent papers from this laboratory,[2] which describe the spectroscopic detection and characterization of the reactive intermediate, $[MeRh(CO)_2I_3]^-$ (**2a**, eq 1). Rhodium/iodide based catalysts also promote the carbonylation of higher alcohols to linear or branched chain carboxylic acids.[3-5] For example, ethanol is converted into propanoic acid, and *n*-propanol yields a mixture of *n*-butanoic and isobutanoic acids. In this paper, we describe the stoichiometric reactions of **1** with higher

$$\underset{\mathbf{1}}{MeI + [Rh(CO)_2I_2]^-} \rightarrow \underset{\mathbf{2a}}{[MeRh(CO)_2I_3]^-} \rightarrow \underset{\mathbf{3a}}{[Rh(CO)(COMe)I_3]^-} \quad (1)$$

[⊗] Abstract published in *Advance ACS Abstracts,* July 1, 1994.

(1) Forster, D. *Adv. Organomet. Chem.* **1979**, *17*, 255. Forster, D.; Singleton, T. C. *J. Mol. Catal.* **1982**, *17*, 299. Dekleva, T. W.; Forster, D. *Adv. Catal.* **1986**, *34*, 81. Howard, M. J.; Jones, M. D.; Roberts, M. S.; Taylor, S. A. *Catal. Today* **1993**, *18*, 325. Eby, R. T.; Singleton, T. C. In *Applied Industrial Catalysis*; Leach, B. E., Ed.; Academic Press: New York, 1983; Vol. 1. Parshall, G. W.; Ittel, S. D. *Homogeneous Catalysis*, 2nd ed.; Wiley-Interscience: New York, 1992.

(2) (a) Haynes, A.; Mann, B. E.; Morris, G. E.; Maitlis, P. M. *J. Am. Chem. Soc.* **1993**, *115*, 4093. Haynes, A.; Mann, B. E.; Gulliver, D. J.; Morris, G. E.; Maitlis, P. M. *J. Am. Chem. Soc.* **1991**, *113*, 8657. (b) Fulford, A.; Hickey, C. E.; Maitlis, P. M. *J. Organomet. Chem.* **1990**, *398*, 311. (c) Hickey, C. E.; Maitlis, P. M. *J. Chem. Soc. Chem. Commun.* **1984**, 1609.

0276-7333/94/2313-3215$04.50/0

Scheme 1. Alternative Pathways in the Carbonylation of Alcohols, ROH (R ≠ Me), to Carboxylic Acids, Catalyzed by $[Rh(CO)_2I_2]^-$

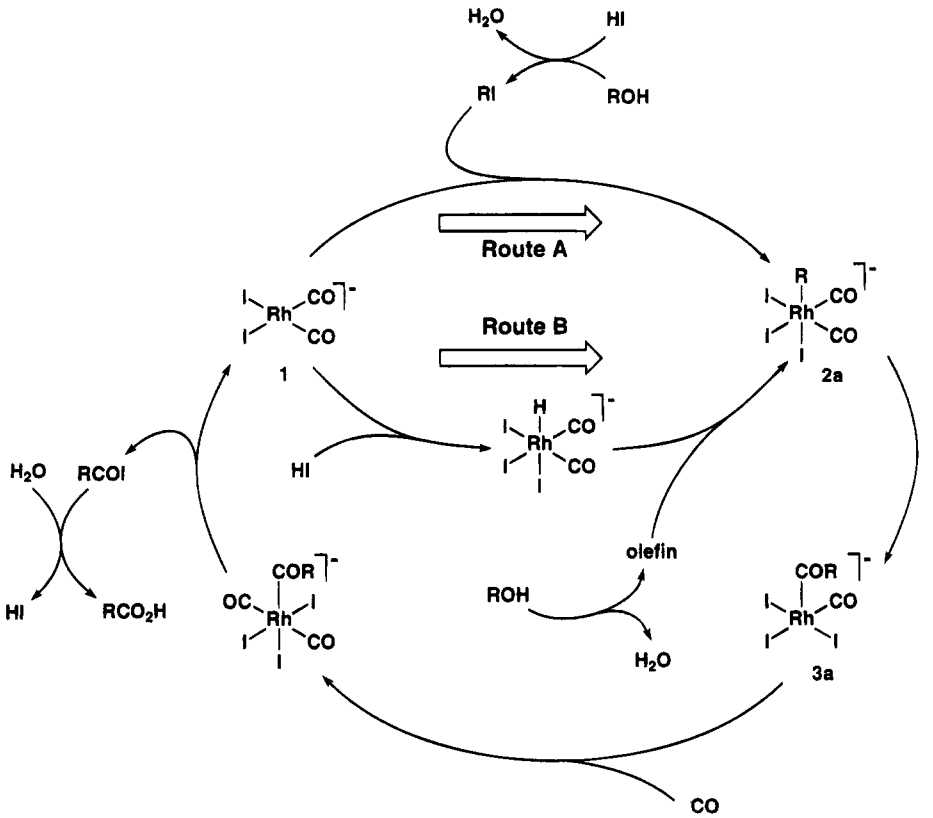

alkyl iodides and discuss the role of these reactions in catalytic alcohol carbonylation.

The route to metal–carbon bond formation in the carbonylation of higher alcohols has been the subject of some debate. The stoichiometry for formation of an alkylrhodium complex from the reaction of **1** with an alcohol and HI is given in eq 2. Two alternative mech-

$$\underset{\mathbf{1}}{[Rh(CO)_2I_2]^-} + ROH + HI = \underset{\mathbf{2}}{[RRh(CO)_2I_3]^-} + H_2O \quad (2)$$

anisms for this reaction are depicted in Scheme 1. Route A involves the initial reaction of the alcohol with HI to give the corresponding alkyl iodide, which undergoes oxidative addition to **1**. This is identical to the mechanism which has been shown to operate in methanol carbonylation. By contrast, route B involves oxidative addition of HI to **1**, giving an intermediate rhodium hydride. In this case the metal alkyl arises by reaction with an *alkene*, formed by dehydration of the alcohol. Route B is similar to the mechanism of alkene hydrocarboxylation promoted by related catalysts.[6] For unsymmetrical alkenes (e.g. propene), route B can directly produce two possible isomeric metal alkyl species, depending on the stereochemistry of insertion, whereas route A can only give isomeric products if subsequent alkyl isomerizations take place, presumably via β-H transfers.

The original studies concluded that oxidative addition of alkyl iodide (route A) is the major pathway for Rh/I^- catalyzed carbonylation of ethanol or *n*-propanol. This conclusion was based on studies of the effect of CO pressure on the isomeric product distributions for carbonylation of *n*-propanol[3a] and of $^{13}CH_3CH_2OH$.[3d] The observed inhibition of alkyl isomerization at high CO pressures was accounted for in terms of competitive carbonylation and alkyl isomerization after rate determining oxidative addition of the alkyl iodide derived from the reactant alcohol. However, stoichiometric reactions of $[Rh(CO)_2I_2]^-$ with higher alkyl iodides have not been reported.

Very recently, Roe et al. have given direct evidence for some of the intermediates depicted in route B of Scheme 1. The rhodium(III) hydrides, $[HRh(CO)_2I_3]^-$ and $[HRh(CO)_2I_2]$, were detected by low temperature ^1H and ^{13}C NMR spectroscopy during the reaction of HI with $[Rh(CO)_2I_2]^-$. Reaction of the hydride species with ethylene yielded the acyl, $[Rh(CO)(COEt)I_3]^-$, presumably via the unobserved $[EtRh(CO)_2I_3]^-$.[7] They also found that $[Rh(CO)_2I_2]^-$ is unreactive toward ethyl iodide at temperatures up to 60 °C. In this paper, we present results which demonstrate that $[Rh(CO)_2I_2]^-$ does react directly with higher alkyl iodides under more forcing conditions and hence that route A is feasible for catalytic alcohol carbonylation.

Systems based on the 5d congener, iridium, are also active for the catalytic carbonylation of alcohols,[1,8] thus

(3) (a) Dekleva, T. W.; Forster, D. *J. Am. Chem. Soc.* **1985**, *107*, 3565. (b) Dekleva, T. W.; Forster, D. *J. Am. Chem. Soc.* **1985**, *107*, 3568. (c) Dekleva, T. W.; Forster, D. *Abstr. Pap.—Am. Chem. Soc.* **1984**, 198th, INDE 0108. (d) Dekleva, T. W.; Forster, D. *J. Mol. Catal.* **1985**, *33*, 269.

(4) Hjortkjaer, J.; Jorgensen, J. C. *J. Chem. Soc., Perkin Trans. 2* **1978**, 763. Hjortkjaer, J.; Jorgensen, J. C. *J. Mol. Catal.* **1978**, *4*, 199.

(5) Dake, S. B.; Kohle, D. S.; Chaudhari, R. V. *J. Mol. Catal.* **1984**, *24*, 99. Dake, S. B.; Chaudhari, R. V. *J. Mol. Catal.* **1986**, *35*, 119.

(6) Forster, D.; Hershman, A.; Morris, D. E. *Catal. Rev.—Sci. Eng.* **1981**, *23*, 89.

(7) Roe, D. C.; Sheridan, R. E.; Bunel, E. E. *J. Am. Chem. Soc.* **1994**, *116*, 1163.

the reactions of alkyl iodides with the isostructural iridium complex, **4**, provide an interesting counterpoint. There are significant differences between the two. For rhodium, oxidative addition of methyl iodide is followed by rapid migratory insertion to give the acyl **3a**, (eq 1) which exists in the solid state as the dimeric dianion $[\{Rh(CO)(COMe)I_3\}_2]^{2-}$. The ease of migration for rhodium means that it is difficult to study the oxidative addition step in isolation. By contrast, oxidative addition of methyl iodide to $[Ir(CO)_2I_2]^-$ (**4**) yields a stable methyliridium complex, **5a**,[9] for which migratory insertion only occurs at elevated temperatures in the presence of carbon monoxide.

$$\underset{\mathbf{4}}{MeI} + [Ir(CO)_2I_2]^- \rightarrow \underset{\mathbf{5a}}{[MeIr(CO)_2I_3]^-} \xrightarrow[\Delta]{CO} [Ir(CO)_2(COMe)I_3]^- \quad (3)$$

The iridium reaction therefore provides a useful model for the more complex rhodium system. We have already reported preliminary kinetic studies which show that the rate of oxidative addition of methyl iodide is more than 2 orders of magnitude faster for iridium than for rhodium.[10] We now present quantitative kinetic data on the reactions of a range of alkyl iodides with both the rhodium and iridium complexes **1** and **4**, together with spectroscopic characterization of the products and an X-ray crystallographic structure determination for the *n*-hexyliridium complex. We also present direct evidence for alkyl group isomerization in both the rhodium and iridium systems, which sheds light on the mechanism of formation of isomeric products in catalytic alcohol carbonylation.

Results

Oxidative Addition of RI to $[Rh(CO)_2I_2]^-$, 1. The anion, $[Rh(CO)_2I_2]^-$ (**1**), is very much less reactive with higher alkyl iodides than with methyl iodide. Preparative and kinetic studies of these reactions were therefore performed at higher temperatures in a stainless steel (Fisher Porter) tube, to exclude light and to avoid loss of RI by volatilization. Thus, reaction of the tetraphenylarsonium salt of **1** with the neat freshly distilled alkyl iodide (80 °C, 5 atm N_2) gave acyl complexes analogous to **3a**:

$$\underset{\mathbf{1}}{RI} + Ph_4As[Rh(CO)_2I_2] \rightarrow \underset{\mathbf{3b-3d}}{Ph_4As[Rh(CO)(COR)I_3]} \quad (4)$$

b, R = Et; **c**, R = ^{n}Pr; **d**, R = ^{i}Pr

The tetraphenylarsonium salts **3b–3d** were isolated as dark red crystals and characterized by microanalysis and spectroscopy. Their IR spectra in CH_2Cl_2 were similar to that of **3a**, with bands at ca. 2060 cm^{-1} (ν(CO), terminal) and ca. 1750 cm^{-1} (ν(CO), acyl). In each case the terminal ν(CO) band exhibited a shoulder to high frequency and the acyl bands were broad (**3c**, **3d**) or split (**3b**), indicating the presence of more than one isomer.[11] The ^{1}H NMR spectra (Table 1) showed the characteristic resonances expected for the acyls. Our spectroscopic data for the propanoyl complex, **3b**, concur with those reported by Roe et al. for the product of the reaction of **1** with HI and ethylene.[7] For simplicity the acyl complexes **3b–3d** are written as $[Rh(CO)(COR)I_3]^-$; however, in the solid and in weakly coordinating solvents such as CH_2Cl_2, they are probably all dimers with bridging iodides and 6-coordinate rhodium, $[\{Rh(CO)(COR)I_3\}_2]^{2-}$, with structures similar to those determined for **3a**.[11]

Table 1. ^{1}H NMR Spectroscopic Data ($CDCl_3$, 250 MHz) for the Alkyl Groups of Rh Acyl Complexes 3b–d and Ir Alkyl Complexes 5b–g[a]

	carbon of alkyl chain to which hydrogens are bonded					
complex	α	β	γ	δ	ϵ	ζ
3b	3.42, q	0.95, t				
3c	3.15, t	1.82, m	0.95, t			
3d	4.40, sept	1.80, d				
5b	2.96, q	1.60, t				
5c	2.97, m	1.79, m	0.89, t			
5d	2.97, sept	1.79, d				
5e	3.03, m	1.80, m	1.29, m	0.97, t		
5f	3.04, m	1.85, m	1.29, m	1.29, m	0.99, t	
5g	3.02, m	1.80, m	1.58, m	1.58, m	1.58, m	0.83, t

Table 2. Microanalytical Data for Tetraphenylarsonium Salts of the Rhodium Acyl Complexes 3b–d and Ir Alkyl Complexes 5b,c,e–g

	% C		% H		% I	
complex	calc	found	calc	found	calc	found
3b	35.3	35.5	2.6	2.4	40.0	40.2
3c	36.1	36.2	2.8	2.6	39.4	39.7
3d	36.1	36.4	2.8	2.7	39.4	39.2
5b	32.3	32.1	2.4	2.4	36.6	36.9
5c	33.0	33.1	2.6	2.6	36.1	36.3
5e	33.7	33.5	2.7	2.6	35.6	35.7
5f	34.4	34.1	2.9	2.9	35.1	35.4
5g	35.0	34.8	3.0	3.1	34.7	34.9

These reactions proceeded smoothly and cleanly at temperatures up to 80 °C with no evidence for alkyl group isomerization. Thus, none of the isobutanoyl isomer **3d** was produced in the reaction of **1** with *n*-propyl iodide and none of the *n*-butanoyl isomer was formed in the reaction of **1** with isopropyl iodide. However, when the reaction of **1** with isopropyl iodide was performed above 80 °C, some of the linear isomerized species, **3c**, was found in addition to the expected branched product, **3d** (see below). A side reaction above 80 °C also leads to formation of some *trans*-$[Rh(CO)_2I_4]^-$ (ν(CO), 2089 cm^{-1}), and above 110 °C, significant decomposition to an insoluble black solid is observed.

Kinetic data for these oxidative addition reactions were obtained by periodic removal of small samples from the reaction vessel for analysis by IR spectroscopy. The reaction was monitored by following the decrease of the low frequency ν(CO) absorption of **1** at 1985 cm^{-1}. The procedure involved a number of transfer operations which, despite our best precautions, led to errors somewhat higher than usual. Nevertheless, plots of A_{1985} vs time followed good exponential decays for the reactions leading to **3b** and **3c**, indicating a first-order dependence on the concentration of **1** (eq 5; M = Rh; k_{obs} is the observed first-order rate constant). By

(8) Forster, D. *J. Chem. Soc., Dalton Trans.* **1979**, 1639. Patil, R. P.; Kelkar, A. A.; Chaudhari, R. V. *J. Mol. Catal.* **1988**, *47*, 87. Patil, R. P.; Kelkar, A. A.; Chaudhari, R. V. *J. Mol. Catal.* **1992**, *72*, 153.
(9) Forster, D. *Inorg. Chem.* **1972**, *11*, 473.
(10) Bassetti, M.; Monti, D.; Haynes, A.; Pearson, J. M.; Stanbridge, I. A.; Maitlis, P. M. *Gazz. Chim. Ital.* **1992**, *122*, 391.
(11) Adamson, G. W.; Daly, J. J.; Forster, D. *J. Organomet. Chem.* **1974**, *71*, C17. Adams, H.; Bailey, N. A.; Mann, B. E.; Manuel, C. P.; Spencer, C. M.; Kent, A. G. *J. Chem. Soc., Dalton Trans.* **1988**, 489.

$$\frac{-d[[M(CO)_2I_2]^-]}{dt} = k_{obs}[[M(CO)_2I_2]^-] \quad (5)$$

contrast, the reaction of **1** with isopropyl iodide gave a poor exponential fit, which was not improved by the addition of a radical scavenger (duroquinone, see below).

In addition to the measurements in neat alkyl iodide, reactions were carried out over a range of alkyl iodide concentrations in chloroform solution at 80 °C. The observed pseudo-first-order rate constants are given in Table 3. The linear plots of k_{obs} vs [RI] (Figure 1) show that the reactions are first-order in [RI]. The fit for isopropyl iodide was significantly poorer than that for the linear alkyl iodides, but even in that case the rate dependence was not unreasonable for a reaction first order in alkyl iodide. The kinetic data therefore suggest that oxidative addition is second-order overall, and $k_{obs} = k_2[RI]$. Values of the second-order rate constant, k_2, obtained from the slopes of plots of k_{obs} vs [RI] at 80 °C are given in Table 3 for each alkyl iodide.

Since the reaction was very sluggish below 70 °C and problems were encountered due to decomposition above 80 °C, the temperature dependence of the reaction rates in neat alkyl iodide could only be measured over a very limited range. Eyring plots of the variable temperature data reported in Table 3 yielded the activation parameters in Table 4.

Oxidative Addition of RI to $[Ir(CO)_2I_2]^-$, 4. Addition of alkyl iodides to $Ph_4As[Ir(CO)_2I_2]$ was much faster than for the rhodium analog and proceeded under mild conditions (30 °C, 16 h, N_2 atmosphere) to give **5b–5g**. As for rhodium, reactions with higher alkyl iodides were much slower than the (already described) reaction with methyl iodide. Indeed, whereas formation of **5a** in neat methyl iodide was complete within seconds, and was too fast to monitor conveniently, the reactions of **4** with neat higher alkyl iodides had half-lives of several hours.

$$RI + \underset{\mathbf{4}}{Ph_4As[Ir(CO)_2I_2]} \rightarrow \underset{\mathbf{5b-g}}{Ph_4As[RIr(CO)_2I_3]} \quad (6)$$

b, R = Et; **c**, R = ^{n}Pr; **d**, R = ^{i}Pr; **e**, R = ^{n}Bu; **f**, R = n-C_5H_{11}; **g**, R = n-C_6H_{13}

All the reactions proceeded cleanly and in high yield except for that with isopropyl iodide, which also gave significant amounts (30–45%) of $Ph_4As[Ir(CO)_2I_4]$ (ν(CO): 2112, 2068 cm^{-1}, CH_2Cl_2). The products were characterized by microanalysis and spectroscopy. In each case the IR spectrum exhibited two strong bands of similar intensity (2094, 2040 cm^{-1}, CH_2Cl_2) in the terminal ν(CO) region, indicative of a *cis*-dicarbonyl geometry. The ν(CO) frequencies for all the higher alkyl complexes are shifted 4–5 cm^{-1} to lower frequency relative to those of the methyliridium complex, **5a** (2098, 2045 cm^{-1}, CH_2Cl_2). The shift can be ascribed to enhanced electron donation from the higher alkyls to iridium. The presence of only one set of resonances in the ^{1}H NMR spectra of the linear alkyl complexes and of two clean ν(CO) bands in the IR spectra indicated the presence of just one geometrical *cis*-dicarbonyl isomer. An X-ray crystal structure determination of the *n*-hexyl derivative **5g**, showed it to have a *fac,cis* stereochemistry, resulting from formal *trans* addition of $C_6H_{13}I$ to the square planar complex **4** (see below).

The ^{1}H NMR spectra of the products from the linear alkyl iodides (Table 1) only showed the presence of the alkyl group derived from the reactant RI; no alkyl group isomerization had occurred. However, some of the *n*-propyl complex, **5c**, was obtained, in addition to **5d**, when the reaction of **4** with isopropyl iodide was carried out at higher temperatures.

Kinetic data were obtained for the reactions of **4** with methyl, ethyl, and *n*-propyl iodides, leading to **5a**, **5b**, and **5c**, respectively. The reactions were monitored by following the decay of the low frequency ν(CO) band of **4** in a thermostated infrared cell. The rate of oxidative addition of methyl iodide to **4** was measured in CH_2Cl_2 at 25 °C as a function of [MeI] (0.08–0.4 M) and at constant [MeI] over the temperature range 5–35 °C. In each experiment the intensity of the ν(CO) absorption of **4** at 1968 cm^{-1} was found to decay exponentially with time, indicating that the reaction rate has a first-order dependence on the concentration of **4**. Observed pseudo-first-order rate constants are given in Table 5. A plot of k_{obs} against the methyl iodide concentration was linear, showing that the reaction is first-order in [MeI] and, hence, second-order overall. Second-order rate constants, k_2(25 °C) are given in Table 5. An Eyring plot of the variable temperature data gave a good straight line, yielding the activation parameters shown in Table 6.

The reactions of **4** with ethyl and *n*-propyl iodides proceeded much more slowly and displayed more complex kinetic behavior. Good exponential decays, consistent with a first-order dependence on [**4**] were observed for experiments performed at 30 °C. However, at higher temperatures, deviations from pseudo-first-order behavior were encountered, both for the decay of the starting material and for the appearance of the high frequency ν(CO) band of the product (2089 cm^{-1}). The reaction rate was found to increase with time, reaching a maximum before decreasing at high conversions, as illustrated by the kinetic trace in Figure 2. These deviations were observed even when light and air were rigorously excluded but were more pronounced when light and air were deliberately admitted, and at higher temperatures. However, repetition of these experiments in the presence of a radical scavenger (duroquinone, 4–5 equiv/Ir) resulted in restoration of simple pseudo-first-order kinetics at all temperatures studied (Figure 2). These observations suggest the participation of a radical process which is suppressed by duroquinone, and therefore all the pseudo-first-order rate constants reported for the reactions of **4** with EtI or ^{n}PrI were measured in the presence of duroquinone. Separate control experiments showed that duroquinone did not react with **4** in either CH_2Cl_2 or acetonitrile (15 h at 30 °C). In contrast, the reaction of **4** with MeI displayed clean pseudo-first-order behavior throughout and identical rates were found both in the presence and in the absence of duroquinone.

Kinetic data for the reactions of **4** with the higher alkyl iodides are given in Table 5. Rate constants were measured both as a function of [RI] in CH_2Cl_2 and as a function of temperature over the range 35–50 °C in the neat alkyl iodide. Plots of k_{obs} vs [RI] are linear (Figure 3), indicating a first-order dependence on alkyl iodide concentration, and hence overall second-order kinetics. Second-order rate constants, k_2(30 °C, CH_2Cl_2) are given

Table 3. Kinetic Data for the Reactions of $Ph_4As[Rh(CO)_2I_2]$ with Alkyl Iodides, RI, in $CHCl_3$ or with the Neat Alkyl Iodide

	R = Et		R = ^{n}Pr		R = ^{i}Pr	
T/°C	[RI]/M	$10^6k_{obs}/s^{-1}$	[RI]/M	$10^6k_{obs}/s^{-1}$	[RI]/M	$10^6k_{obs}/s^{-1}$
70	12.50	15	10.25	7	10.02	17
75	12.50	22	10.25	9	10.02	24
80	12.50	27	10.25	12	10.02	32
80	9.38	22	7.69	9	7.52	20
80	6.25	12	5.13	6	6.01	15
80	3.13	7	2.56	3	5.01	11
80					2.51	7
80	$k_2 = 2.2 \times 10^{-6}\ M^{-1}\ s^{-1}$		$k_2 = 1.2 \times 10^{6}\ M^{-1}\ s^{-1}$		$k_2 = 3.2 \times 10^{-6}\ M^{-1}\ s^{-1}$	

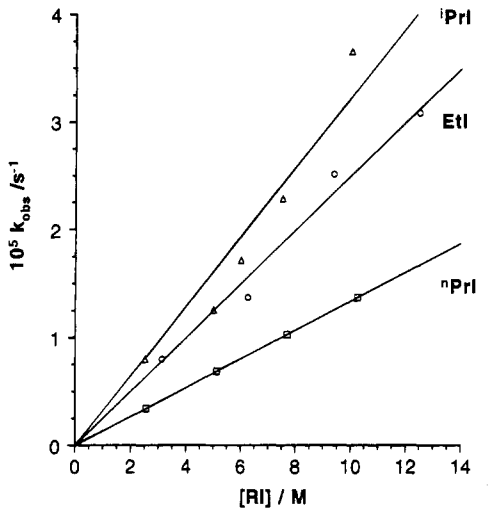

Figure 1. Plots of the observed pseudo-first-order rate constant, k_{obs}, vs the alkyl iodide concentration for the reactions of $Ph_4As[Rh(CO)_2I_2]$ with ethyl, *n*-propyl, and isopropyl iodides in $CHCl_3$ at 80 °C.

Table 4. Activation Parameters for the Reactions of Alkyl Iodides with $Ph_4As[Rh(CO)_2I_2]$[a]

	oxidative addition of RI			catalytic carbonylation of alcohols, ROH[3a]	
R	$\Delta H^{\ddagger}$/kJ mol^{-1}	$\Delta S^{\ddagger}$/J mol^{-1} K^{-1}	$\Delta G^{\ddagger}$(353 K)/kJ mol^{-1}	$\Delta H^{\ddagger}$/kJ mol^{-1}	$\Delta S^{\ddagger}$/J mol^{-1} K^{-1}
Me	50(±1)	−165(4)	108	63.6	−116
Et	56(±10)	−195(25)	125	76.4	−111
^{n}Pr	51(±10)	−215(25)	127	79.5	−109
^{i}Pr	61(±15)	−180(30)	124		

[a] Values of $\Delta G^{\ddagger}$(353 K) were calculated from the measured rate constants at this temperature except that for R = Me which was calculated from values of $\Delta H^{\ddagger}$ and $\Delta S^{\ddagger}$.[2a] Data reported in the literature for Rh/I^- catalyzed alcohol carbonylation are included for comparison.[3a]

in Table 5. Linear Eyring plots of the variable temperature data yielded the activation parameters in Table 6.

X-ray Crystal Structure Determination for $Ph_4As[(n\text{-}C_6H_{13})Ir(CO)_2I_3]$ (5g). Attempted X-ray structure determinations of crystals of $Ph_4As[MeIr(CO)_2I_3]$ were frustrated by disorder between inequivalent iodides in the octahedral complex. However, a structure has been determined for a crystal of the *n*-hexyliridium species, **5g**, grown from a solution of the salt in CH_2Cl_2/Et_2O (Table 7). The structure of the molecular anion is illustrated in Figure 4 and selected bond lengths and angles for **5g** are given in Table 8. The anion comprises an octahedrally coordinated iridium(III) with a facial set of three iodine ligands (mean I—Ir—I angle 92.1°), two carbonyl ligands, and an *n*-hexyl chain. The Ir—I bond *trans* to the alkyl ligand (Ir—I 2.775(4) Å) is significantly longer than the two Ir—I bonds *trans* to the carbonyls (2.701(4), 2.710(4) Å); this is due to the *trans* influence of the *n*-hexyl ligand. In view of the constraints applied during refinement, the geometries of the carbonyls and of the *n*-hexyl ligand cannot be sensibly discussed, but interligand angles of this facial set are also close to 90°. The tetraphenylarsonium cation has the expected approximately tetrahedral geometry, and there are no significant nonbonded contacts.

The crystal structure of **5g** is the first for an anionic iridium—iodo carbonyl complex. The structure of the neutral complex, $IrI(Me)(CF_3)(CO)(PPh_3)_2$,[12] shows that the Ir—I bond (2.785(2) Å) *trans* to the methyl is similar to the Ir—I bond of **5g** *trans* to the hexyl chain (2.775(4) Å), and the Ir—C(methyl) bond of $IrI(Me)(CF_3)(CO)(PPh_3)_2$ (2.12(3) Å) is not significantly different from the Ir—C(27) distance of (2.04(6) Å) in **5g**.

Alkyl Group Isomerization in Rhodium Acyl and Iridium Alkyl Complexes. Under certain conditions, reactions of 2-iodopropane with **1** or **4** resulted in the formation of metal complexes containing *n*-butanoyl (Rh) or *n*-propyl (Ir) ligands, arising from alkyl group isomerization. For example, when the reaction of ^{i}PrI with **1** was carried out above 80 °C, a mixture of the linear and branched butanoyl complexes, **3c** and **3d**, was formed.

Further experiments have been carried out in order to shed light on the mechanism of isomerization. It was found that heating the isobutanoyl complex **3d** in diphenyl ether for 8 h at 100 °C gave the *n*-butanoyl complex **3c** as the only Rh—acyl species detectable by ^{1}H NMR spectroscopy. Identical treatment of **3c** did not result in formation of detectable quantities of **3d**, indicating that the linear species **3c** is thermodynamically favored. No *n* to iso isomerization was observed over 8 h at 80 °C, explaining the selectivity of the oxidative addition reactions at this temperature.

A common mechanism for alkyl isomerization at transition-metal centers is via hydrido-η^2-alkene intermediates. We have therefore studied the reactivity of rhodium acyl complexes toward alkenes under conditions where alkyl isomerization occurs. In each experiment the rhodium complex was heated in diphenyl ether at 100 °C for 8 h in the presence of free alkene. These experiments (Scheme 2) show that in the presence of added ethylene, the isobutanoyl complex, **3d**, gives both the isomerized *n*-butanoyl complex, **3c**, and the propanoyl complex **3b**. More **3b** and less **3c** was produced at higher pressures of ethylene. Similarly, treatment of **3b** with propene resulted in formation of **3c**. Thus, added alkenes are hydrocarbonylated into rhodium acyl complexes under the conditions where isomerization occurs. In addition, ca. 20% of complex **1** was also

(12) Brothers, P. J.; Burrell, A. K.; Clark, G. R.; Rickard, C. E. F.; Roper, W. R. *J. Organomet. Chem.* **1990**, *394*, 615.

Table 5. Kinetic Data for the Reactions of $Ph_4As[Ir(CO)_2I_2]$ with Alkyl Iodides, RI, in CH_2Cl_2 or with the Neat Alkyl Iodide

R = Me			R = ^{n}Pr			R = ^{i}Pr		
T/°C	[RI]/M	$10^3k_{obs}/s^{-1}$	T/°C	[RI]/M	$10^5k_{obs}/s^{-1}$	T/°C	[RI]/M	$10^5k_{obs}/s^{-1}$
5	0.32	0.19	30	12.5	12.2	30	7.69	2.6
15	0.32	0.47	30	9.38	9.5	30	6.41	2.1
25	0.08	0.25	30	6.25	6.7	30	5.13	1.6
25	0.16	0.53	30	3.13	3.1	30	2.56	0.9
25	0.24	0.74	35	12.5	20	35	10.25	4.8
25	0.32	0.99	40	12.5	31	40	10.25	7.6
25	0.40	1.25	45	12.5	46	45	10.25	11
35	0.32	2.05	50	12.5	66	50	10.25	17
25	$k_2 = 3.12 \times 10^{-3}$ M^{-1} s^{-1}		30	$k_2 = 1.00 \times 10^{-5}$ M^{-1} s^{-1}		30	$k_2 = 0.33 \times 10^{-5}$ M^{-1} s^{-1}	

Table 6. Activation Parameters for the Oxidative Addition Reactions of $[Ph_4As][Ir(CO)_2(I)_2]$ with Neat Ethyl and *n*-Propyl Iodides (in the Presence of Duroquinone) and with Methyl Iodide (in CH_2Cl_2)

RI	$\Delta H^{\ddagger}$/kJ mol^{-1}	$\Delta S^{\ddagger}$/J mol^{-1} K^{-1}	$\Delta G^{\ddagger}$(303 K)/kJ mol^{-1}
MeI	54(±1)	−113(±4)	88
EtI	66(±5)	−123(±15)	103
^{n}PrI	66(±3)	−132(±11)	106

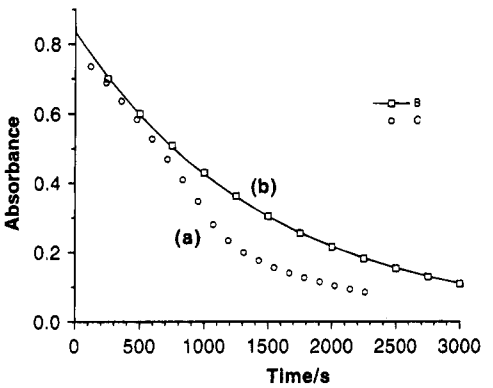

Figure 2. Plots of the IR absorbance (1963 cm^{-1}) against time for the reaction of $Ph_4As[Ir(CO)_2I_2]$ with neat ethyl iodide at 50 °C (a) in the absence of radical scavenger and (b) in the presence of duroquinone (5 equiv/Ir). Note the good exponential fit to the data indicating pseudo-first-order kinetic behavior on addition of the radical scavenger.

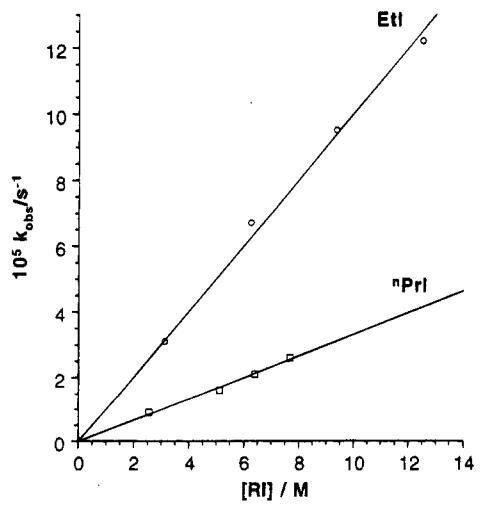

Figure 3. Plots of the observed pseudo-first-order rate constant, k_{obs}, vs the alkyl iodide concentration for the reactions of $Ph_4As[Ir(CO)_2I_2]$ with ethyl and *n*-propyl iodides in CH_2Cl_2 at 30 °C.

produced in each of the reactions shown in Scheme 2; this resulted from elimination of propyl iodide, or of propene and HI, from the metal complex.

Alkyl isomerization was also observed in the iridium system. When the reaction of neat ^{i}PrI with **4** was carried out at 50 °C (5 h) the ^{1}H NMR spectrum of the product exhibited resonances due to both the *n*-propyl complex, **5c**, and the expected isopropyl complex, **5d**. Integration of the NMR signals gave the ratio of isomers **5c**:**5d** of 1:20, corresponding to ca. 5% alkyl group isomerization. When the reaction was repeated at 66 °C, the only alkyliridium species observed after 2 h was the *n*-propyl complex, **5c**, indicating *complete* isomerization under these conditions. When the oxidative addition of ^{i}PrI to **4** was performed at 75 °C under 1 atm of carbon monoxide, the product obtained after 4 h exhibited IR absorptions at 2104, 2065, and 1660 cm^{-1}, closely resembling the spectra of the iridium acyl anions $[Ir(CO)_2(COR)I_3]^-$ which are obtained on heating the alkyls, $[RIr(CO)_2I_3]^-$, in the presence of CO. The ^{1}H NMR spectrum of the product revealed two septets (δ

Table 7. Atom Coordinates ($\times 10^4$)[a] and Temperature Factors (Å^2 × 10^3)

atom	x	y	z	U_{eq}[b]
Ir(1)*	27249(16)	24737(9)	6816(9)	65(1)
I(1)*	−1051(28)	22402(14)	4452(15)	73(1)
I(2)*	25072(32)	37738(17)	990(18)	99(1)
I(3)*	24399(31)	30003(19)	19467(16)	94(1)
As(1)*	42527(35)	44069(18)	−21103(19)	48(1)
O(1)*	59317(16)	27100(9)	9307(9)	108(10)
O(2)*	29058(16)	18754(9)	−7517(9)	210(20)
C(1)	4408(26)	4862(14)	−2956(13)	63(16)
C(2)	4914(26)	5534(14)	−2981(13)	88(21)
C(3)	4912(26)	5873(14)	−3611(13)	100(23)
C(4)	4404(26)	5539(14)	−4216(13)	127(20)
C(5)	3898(26)	4867(14)	−4190(13)	133(29)
C(6)	3899(26)	4529(14)	−3560(13)	85(14)
C(7)	3220(26)	3587(12)	−2210(13)	68(16)
C(8)	3812(26)	3075(12)	−2596(13)	61(15)
C(9)	3073(26)	2462(12)	−2732(13)	168(37)
C(10)	1744(26)	2361(12)	−2483(13)	108(25)
C(11)	1153(26)	2873(12)	−2097(13)	128(19)
C(12)	1891(26)	3486(12)	−1960(13)	91(14)
C(13)	5952(25)	4184(16)	−1683(13)	60(15)
C(14)	6263(25)	3535(16)	−1406(13)	85(20)
C(15)	7622(25)	3394(16)	−1094(13)	79(18)
C(16)	8671(25)	3902(16)	−1059(13)	108(27)
C(17)	8361(25)	4551(16)	−1336(13)	131(31)
C(18)	7002(25)	4692(16)	−1648(13)	92(21)
C(19)	3306(24)	5033(11)	−1563(12)	40(8)
C(20)	2025(24)	5313(11)	−1850(12)	97(21)
C(21)	1265(24)	5769(11)	−1470(12)	67(12)
C(22)	1785(24)	5945(11)	−802(12)	122(28)
C(23)	3065(24)	5665(11)	−515(12)	121(26)
C(24)	3826(24)	5209(11)	−895(12)	75(17)
C(25)*	47227(16)	26208(9)	8367(9)	66(11)
C(26)*	28376(16)	21010(9)	−2112(9)	99(15)
C(27)	2925(50)	1554(29)	1186(27)	148(33)
C(28)	4229(61)	1172(21)	954(31)	321(80)
C(29)	4537(64)	533(21)	1405(29)	439(104)
C(30)	3742(47)	−91(20)	1081(26)	139(41)
C(31)	4371(69)	−757(20)	1407(29)	199(32)
C(32)	3795(67)	−1378(21)	984(35)	243(54)

[a] The x, y, z values for atoms marked with an asterisk are $\times 10^5$. [b] Equivalent isotropic U defined as one-third of the trace of the orthogonalized U_{ij} tensor.

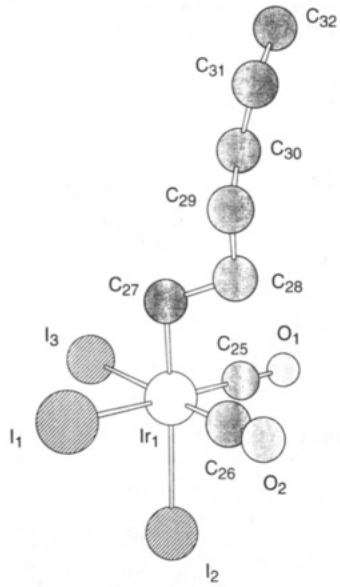

Figure 4. X-ray crystal structure showing the *fac,cis* geometry of the octahedral iridium anion in $Ph_4As[(n\text{-}C_6H_{13})Ir(CO)_2I_3]$. The tetraphenylarsonium cation has been removed for clarity.

Table 8. Selected Bond Lengths (Å) and Angles (deg) for $[Ph_4As][Ir(CO)_2(I)_3(^nC_6H_{13})]$

Ir(1)—I(1)	2.701(4)	Ir(1)—I(2)	2.775(4)
Ir(1)—I(3)	2.710(4)	Ir(1)—C(27)	2.044(55)
I(1)—Ir(1)—I(2)	92.7(1)	I(1)—Ir(1)—I(3)	92.6(1)
I(2)—Ir(1)—I(3)	91.1(1)	I(1)—Ir(1)—C(25)	178.8(1)
I(2)—Ir(1)—C(25)	88.0(1)	I(3)—Ir(1)—C(25)	88.4(1)
I(1)—Ir(1)—C(26)	84.9(1)	I(2)—Ir(1)—C(26)	88.9(1)
I(3)—Ir(1)—C(26)	177.5(1)	I(2)—Ir(1)—C(27)	175.3(15)
I(1)—Ir(1)—C(27)	89.0(13)		

4.30 and 4.00) and two doublets (δ 1.80 and 1.20), consistent with the presence of two inequivalent isopropyl moieties. The spectroscopic data are therefore consistent with formation of two isomers of the isobutanoyl complex $[Ir(CO)_2(CO^iPr)I_3]^-$. None of the corresponding *n*-butanoyl complex was detected under these conditions.

Discussion

Oxidative Addition to $[Rh(CO)_2I_2]^-$, 1. We have shown that the reactions of higher alkyl iodides with the rhodium and iridium anions, **1** and **4**, are analogous to those with methyl iodide. Reactions of $[Rh(CO)_2I_2]^-$ (**1**) with the higher alkyl iodides proceeded cleanly at or below 80 °C, although side reactions were observed at higher temperatures. The products are acyl complexes, $[Rh(CO)(COR)I_3]^-$ (**3**), resulting from oxidative addition followed by intramolecular migratory CO insertion. In the solid state and in weakly coordinating solvents it is likely that the coordinative unsaturation of these 16e species is relieved by dimerization through Rh—I—Rh bridges, as demonstrated for the methyl analog, **3a**.[11] Alkylrhodium intermediates, analogous to the methylrhodium species **2a**, which we detected spectroscopically during the reaction of **1** with MeI,[2a] could not be seen for the higher alkyls, presumably due to their much smaller steady state concentrations, arising from the much slower reactions. The relatively high temperatures required for these reactions explain why Roe et al. did not observe a reaction between **1** and EtI at 60 °C.[13]

Kinetic measurements show that the reactions are first-order in both [**1**] and [RI]. We make the approximation that k_2, the measured second-order rate constant for the net reaction

$$\mathbf{1} + \mathrm{RI} \rightarrow \mathbf{3}$$

is the rate constant for the initial oxidative addition step. This assumes that alkyl migration is fast relative to reductive elimination of RI from the alkylrhodium intermediate, in agreement with our finding that migratory insertion is one order of magnitude faster than loss of MeI from $[MeRh(CO)_2I_3]^-$.[2a] Hence $k_{2(Rh)}$ is dominated by the oxidative addition step and may usefully be compared to $k_{2(Ir)}$.

Oxidative Addition to $[Ir(CO)_2I_2]^-$, 4. Spontaneous alkyl migration did not occur in the iridium system and stable complexes $[RIr(CO)_2I_3]^-$ (**5**) were isolated. A crystal structure determination for the *n*-hexyl anion **5g** shows it to have the same *fac,cis* octahedral geometry to that suggested, on spectroscopic evidence, for the unstable methylrhodium species, **2a**.[2a] Since the M—C bonds are thus in the same environments in the two complexes, the easier migration which occurs for rhodium may be a consequence of the relative strengths of the M—C bonds. Although no data are available for rhodium and iridium, bonds to 5d elements are generally stronger than those to the corresponding 4d metal.[14] This also implies significant weakening of the M—C bond in the transition state for migration.

Although clean second-order kinetics were observed for the reaction of the iridium complex **4** with MeI, those of **4** with EtI and ^{n}PrI exhibited a more complex kinetic behavior, with substantial deviations from pseudo first order, particularly in the presence of light or air, and at higher temperatures. Addition of a radical scavenger (duroquinone, 4–5 equiv/Ir) resulted in restoration of simple pseudo-first-order kinetics, suggesting that the complex rate behavior is due to a radical process which competes with the second-order reaction. We estimate that the radical component accounts for ca. 20% of the overall reaction of **4** with ethyl iodide at 50 °C.

The participation of radicals in oxidative addition to Ir(I) is well documented,[15] and radical chain processes have been suggested to account for certain aspects of the reactions of Vaska complexes, $Ir(CO)Cl(PR_3)_2$, with alkyl halides. The propagation steps in the proposed mechanism involve capture of alkyl radicals by the Ir^I complex, followed by rate determining abstraction of an iodine atom from RI by the intermediate Ir^{II} species:

$$R^\bullet + Ir^I \rightarrow R{-}Ir^{II}$$

$$R{-}Ir^{II} + R{-}I \rightarrow R{-}Ir^{III}{-}I + R^\bullet$$

We suggest that similar steps may occur in the reaction of **4** with the higher alkyl halides. Several Ir-

(13) Roe et al.[7] reported that $[Rh(CO)_2I_2]^-$ did not react with EtI (the solvent and concentration were unspecified) over 24 h at 60 °C. Our data predict a half-life of ca. 21 h for the reaction of $[Rh(CO)_2I_2]^-$ with *neat* EtI at 60 °C.

(14) Mancuso, C.; Halpern, J. *J. Organomet. Chem.* **1992**, *428*, C8.

(15) See, for example: Labinger, J. A.; Osborn, J. A. *Inorg. Chem.* **1980**, *19*, 3230. Labinger, J. A.; Osborn, J. A.; Coville, N. J. *Inorg. Chem.* **1980**, *19*, 3236. Jensen, F. R.; Knickel, B. *J. Am. Chem. Soc.* **1971**, *93*, 6339.

Scheme 2. Product Distributions (±5%) for Alkyl Isomerization and Alkene Incorporation Reactions of Rhodium Acyl Complexes 3b and 3d

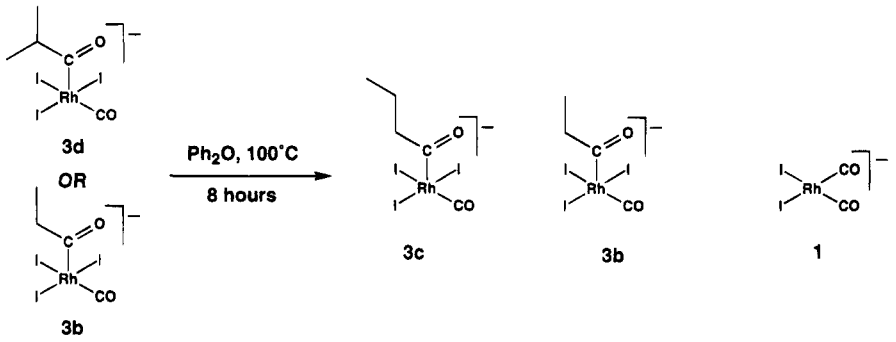

Starting complex	Conditions		Product Distribution (%)	
3d	1 atm N_2	80	0	20
3d	1 atm C_2H_4	20	60	20
3d	5 atm C_2H_4	5	75	20
3b	1 atm C_3H_6	80	0	20

(II) carbonyl halide complexes have been prepared,[16] and thus there is ample precedent for such an oxidation state as an intermediate. The generation of alkyl radicals from RI may be promoted thermally, since we see larger deviations from pseudo-first-order behavior at higher temperatures. However, our evidence suggests that radical initiation can also arise through air oxidation or by photochemical means since we find that both adventitious oxygen and light can affect the kinetics. Oxidation of 4 would lead to an Ir(II) species which could generate alkyl radicals by abstraction of iodine from RI. The alkyl radical can then enter the propagation steps shown above.

$$Ir^{I} - e^{-} \rightarrow Ir^{II}$$

$$Ir^{II} + R{-}I \rightarrow Ir^{III}{-}I + R^{\bullet}$$

In contrast to the iridium system anomalous kinetic behavior was not observed for oxidative addition of linear alkyl iodides to $[Rh(CO)_2I_2]^-$ (**1**). This may well correlate with the greater reluctance of rhodium carbonyl halides to form Rh(II) species; it has previously been noted that iridium complexes are more prone to undergo single electron transfer reactions than their rhodium analogs.[17]

Mechanism of Oxidative Addition and the Effect of the Alkyl Group. Most of the reactions investigated were first-order in both $[M(CO)_2I_2]^-$ and the alkyl iodide, indicating that the slow rate determining step is bimolecular. The activation parameters listed in Tables 4 and 6 have the common feature of a large negative entropy of activation, suggesting a highly ordered transition state, consistent with these reactions proceeding by an S_N2 mechanism, as proposed for the reaction with MeI. Relative rate data for the reactions of **1** and **4** with different alkyl iodides are given in Table IX. For rhodium, comparison was achieved by calculating a value of the rate constant at 80 °C for MeI, using activation parameters obtained in a prior study[2a] (k_2(MeI) = 7.1×10^{-4} M^{-1} s^{-1}, 80 °C). This is considered more reliable than extrapolation to lower temperatures for the higher alkyl iodides, due to relatively large errors in the activation parameters obtained for those reactions.

Table 9. Relative Rates for the Reactions of 1 and 4 with Different Alkyl Iodides[a]

			relative rates					
nucleophile	*T*/°C	solvent	MeI	EtI	^{n}PrI	^{i}PrI	^{n}Bu	ref
1	80	RI	1000	3	1.7	4		
4	30	CH_2Cl_2	1000	2.3	0.75			
$CpCo(CO)(PPh_2Me)$	25	CH_2Cl_2	1000	2				18a
$CpCo(CO)(PPh_3)$	25	CH_2Cl_2	1000	2.5				18a
$CpRh(CO)(PPh_3)$	25	CH_2Cl_2	1000	0.8				18a
$CpIr(CO)(PPh_3)$	25	CH_2Cl_2	1000	1				18a
$Me_2Pt(phen)$	25	Me_2CO	1000	1	0.5		0.6	18b
vitamin B_{12}	25	MeOH	1000	9.4	7.2		5.6	18c
I^-	50	acetone	1000	12.5	5.5		5.0	19
organic S_N2			1000	33	13	0.8	13	20

[a] Comparative data are given for other transition metal nucleophiles and the iodide anion. For each nucleophile, the rates are scaled relative to that for reaction with the methyl halide, set arbitrarily to 1000. Note that the relative rates quoted for vitamin B12 and the iodide anion refer to the reactions with the alkyl *chlorides*. The bottom row of the table gives typical relative rates for organic S_N2 reactions.

For both metals the largest difference in reaction rate is observed between MeI and EtI, with much smaller changes on further increases in the alkyl chain length. On the basis of a relative rate of 1000 for MeI, EtI is 3 for Rh and 2.3 for Ir, these values fall into the range reported for other transition-metal complexes[18] (Table 9), where it can be seen that MeI is a factor of 10^2–10^3 more reactive than EtI. Non-transition-metal nucleophiles, such as the iodide anion[19] and organic amines,[20] also exhibit a large step change in reactivity between

(16) Angoletta, M. *Gazz. Chim. Ital.* **1960**, *93*, 1591. Teo, B-K.; Snyder-Robinson, P. A. *J. Chem. Soc., Chem. Commun.* **1979**, 255. Bonnet, J-J.; Kalck, P.; Poilblanc, R. *Angew. Chem., Int. Ed. Engl.* **1980**, *19*, 551.

(17) Chanon, M. *Bull. Soc. Chim. Fr.* **1982**, II-197.

(18) (a) Hart-Davis, A. J.; Graham, W. A. G. *Inorg. Chem.* **1970**, *9*, 2658. (b) Monaghan, P. K.; Puddephatt, R. J. *J. Chem. Soc., Dalton Trans.* **1988**, 595. (c) Schrauzer, G. N.; Deutsch, E. *J. Am. Chem. Soc.* **1968**, *90*, 2441.

(19) Hine, J. *Physical Organic Chemistry*; McGraw-Hill: New York, 1962; p 176.

(20) March, J. *Advanced Organic Chemistry*, 4th ed.; J. Wiley: New York, 1992; p 339 et seq.

MeI (1000) and EtI(33), although the effect is somewhat less pronounced. The similarity in reactivity trends for all these reactions supports the proposal that oxidative addition to **1** and **4** proceeds by a classic S_N2 process at carbon, as previously suggested for addition of MeI. The larger difference in reactivity between methyl and longer alkyl iodides exhibited by metal complexes by comparison with organic nucleophiles, is probably due to increased steric congestion around the metal center.

One apparent anomaly in our data is that the reaction of **1** with ^{i}PrI is faster than those with EtI and ^{n}PrI. For an S_N2 process, steric effects at the carbon undergoing substitution should result in decreased reactivity for secondary compared with primary alkyl substrates. Thus our data for the rhodium system cannot be completely described in terms of classical S_N2 reactivity trends, and it is likely that an additional pathway (which could also account for the observed deviations from clean second-order kinetics) is available for the branched alkyl iodide. This might be some type of radical process, possibly involving caged species, since addition of duroquinone had no effect.

The slower rates for reactions of **1** with higher alkyl iodides reflect an increase of 16–19 kJ mol^{-1} in $\Delta G^{\ddagger}$(353 K) compared to the reaction with MeI. Due to the relatively large errors in activation parameters for the rhodium system, we are unable to distinguish between enthalpic or entropic origins for this increase. However, more accurate activation parameters for the iridium system suggest that increases in $\Delta G^{\ddagger}$(303 K) of 15 kJ mol^{-1} between MeI and EtI and a further 3 kJ mol^{-1} between EtI and ^{n}PrI are mainly a result of an increase in $\Delta H^{\ddagger}$. This would appear to be in conflict with the measured C–I bond dissociation energy, which is actually *greater* for Me–I (234 kJ mol^{-1}) than for Et–I (224 kJ mol^{-1}).[21] However, $\Delta H^{\ddagger}$ will include a contribution from a stabilizing M–C interaction in the transition state, which is expected to be smaller for more sterically demanding alkyls. Steric hindrance may also affect solvation of the transition state.

Relative Rates for Rhodium and Iridium. The relative reactivities of the rhodium anion **1** and the iridium anion **4** toward each of the three different alkyl iodides are roughly the same. For example, extrapolation to 80 °C using the activation parameters obtained for each system gives values of k_{Ir}/k_{Rh} of ca. 150 (R = Me), 220 (R = Et), and 140 (R = ^{n}Pr). This similarity is not unexpected: Rh and Ir are very similar in size and thus the steric requirements of the two nucleophiles will be the same. The major determining factor is therefore likely to be the different degrees of steric hindrance at the electrophilic center, the carbon bearing the iodine. The higher nucleophilicity of iridium complexes compared to their rhodium analogs has been noted previously;[22] it has been suggested that relativistic effects for the third transition series lead to radial expansion and energetic destabilization of the 5d compared with the 4d orbitals.[23]

Alkyl Isomerization. Our successful preparation of higher alkyl congeners of the well established rhodium acetyl and iridium methyl complexes **3a** and **5a** has allowed us to probe the mechanism of alkyl group isomerization in catalytic alcohol carbonylation. Such isomerization was evident in the formation of mixtures of the linear and branched butanoylrhodium complexes, **3c** and **3d**, on reaction of **1** with ^{i}PrI at temperatures above 80 °C. Separate experiments have shown that ^{i}PrI itself is not converted into ^{n}PrI under these conditions and, since we find that the branched butanoyl complex, **3d**, is converted into the thermodynamically preferred linear complex, **3c**, at 100 °C, isomerization must be able to occur subsequent to the initial oxidative addition and migratory insertion reactions. Roe et al. reported that the reverse isomerization, **3c** → **3d**, can also occur in acetonitrile solvent at 40 °C.[7] Under those conditions an equilibrium was attained which favored the *n*-butanoyl complex (**3c**:**3d** = 2:1).[24] It therefore appears that the position of equilibrium between *n*-butanoyl and isobutanoyl complexes varies with both temperature and solvent. The effect of reaction conditions on both the kinetics and thermodynamics of isomerization is of considerable interest and will be the subject of further research.

Scheme 3. Mechanism for Alkyl Group Isomerization and Alkene Incorporation Reactions of Rhodium Acyl Complexes 3b–d[a]

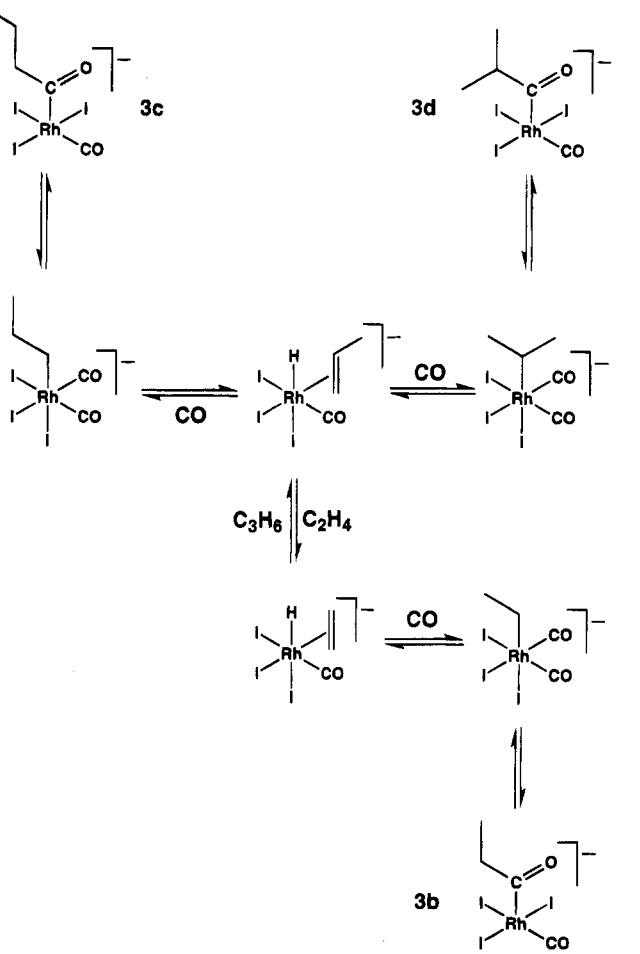

[a] Note that β-H transfer to generate η^2-alkene complexes may be facilitated by dissociation of an iodide ligand, as an alternative to the CO-loss mechanism illustrated.

A mechanism for isomerization is illustrated in the upper portion of Scheme 3. Starting from complex **3d**, the first step involves migration of the isopropyl moiety

(21) Lowry, T. H.; Richardson, K. S. *Mechanism and Theory in Organic Chemistry*, 3rd ed.; Harper and Row: New York, 1987; p 161.
(22) Henderson, S.; Henderson, R. A. *Adv. Phys. Org. Chem.* **1987**, *23*, 1.
(23) Pyykko, P. *Chem. Rev.* **1988**, *88*, 563.
(24) Bunel, E. E. Personal communication.

Scheme 4. Competitive Reaction Pathways for the isopropyliridium Complex, 5d, in the Presence or Absence of Carbon Monoxide

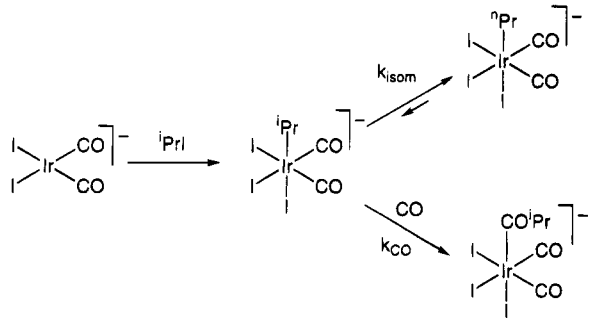

from carbonyl to rhodium. Isotopic labeling experiments in our laboratory recently demonstrated that such carbonyl deinsertion (reverse migration) occurs for the methyl analog.[2a] The activation parameters obtained can be used to predict a half-life of ca. 16 s for deinsertion at 100 °C. The next step involves β-H transfer to rhodium. This requires a vacant coordination site, created by loss of a carbonyl (or iodide) ligand. The intermediate hydrido alkene complex can undergo alkene insertion to give either the linear or branched alkyl complex, explaining the observed isomerization.

Convincing evidence for a hydrido–alkene intermediate was obtained by treating the rhodium acyls with added alkene under conditions where isomerization occurs. Thus, the isobutanoyl complex, **3d**, gives both **3c** and **3b** in the presence of ethylene. Formation of the propanoyl complex, **3b**, is accounted for by exchange of propylene for ethylene in a hydrido–alkene intermediate. The reverse process was also observed, whereby addition of propylene to **3b** leads to formation of **3c**. The thermodynamic preference for linear alkyl species is presumably due to steric congestion in the butanoyl rhodium triiodide carbonyl systems.

Comparable isomerizations of platinum group metal acyl complexes were reported by Brumbaugh and Sen.[25] Palladium acyls, $[Pd(PPh_3)_2(MeCN)(COR)]^+$ (R = ^{i}Pr, ^{s}Bu, ^{t}Bu), were found to undergo spontaneous alkyl isomerization, leading to an equilibrium mixture favoring species with less branching in the alkyl chain. Incorporation of added alkene was also observed in these systems, and a mechanism involving successive carbonyl deinsertion and β-H transfer steps was proposed.

Alkyl isomerization was also evident in the products of oxidative addition of ^{i}PrI to the iridium anion, **4**. Increased quantities of the *n*-propyl complex **5c** relative to the isopropyl complex, **5d**, were obtained when the reaction was carried out at higher temperatures. However, when ^{i}PrI was reacted with **4** under a carbon monoxide atmosphere at 75 °C, only the isobutanoyl complex, $[Ir(CO)_2(CO^iPr)I_3]^-$, was formed. These observations can be explained by the competing reactions shown in Scheme 4. Oxidative addition of ^{i}PrI to **4** yields the isopropyliridium complex, **5d**, as the primary product. At elevated temperatures alkyl isomerization can occur, resulting in conversion of **5d** into the thermodynamically favored linear alkyl complex, **5c**, but in the presence of 1 atm of carbon monoxide, **5d** is trapped by carbonylation to give only isobutanoyl species (i.e. $k_{CO}[CO] \gg k_{isom}$). There are two alternative explanations for the inhibition of isomerization by carbon monoxide: (i) k_{isom} is reduced, due to a smaller steady state concentration of coordinatively unsaturated monocarbonyl species in which β-H transfer can occur; (ii) k_{isom} is unaffected, but CO-induced alkyl migration is fast enough to effectively trap the isopropyl intermediate.

Bennett et al. have reported alkyl isomerizations in closely related *neutral* alkyliridium carbonyl halides.[26] A 3:2 equilibrium mixture of *n*-propyl and isopropyl complexes was generated on heating either of the dimers $[^nPrIr(CO)_2Cl_2]_2$ and $[^iPrIr(CO)_2Cl_2]_2$ in benzene. Again, linear alkyl complexes were favored thermodynamically, but to a smaller extent than in our studies, because of the less demanding steric requirements of chloride compared to iodide ligands. This argument is supported by Bennett's observation of complete isomerization to linear alkyls in the more sterically crowded bis(phosphine) complexes, $[RIr(CO)(PR'_3)_2ClY]$ (PR'_3 = PPh_3, $PMePh_2$, PMe_3; Y = Cl, I)[26a–c] and $[RIr(Me)(CO)(PMe_3)_2X]$ (X = Br, I).[26d] In these cases it was shown that dissociation of a halide ligand generates the vacant coordination site required for β-H transfer; this mechanism may also operate in our anionic systems.

Relevance of Results to Catalytic Alcohol Carbonylation. The relative rates for reaction of alkyl halides with **1** (Table 9) correlate reasonably well with the relative rates for the rhodium catalyzed carbonylation of the corresponding alcohols, (1000 (MeOH), 48 (EtOH), 22 (^{n}PrOH), 57–180 (^{i}PrOH) at 170 °C and 35 atm of CO). The principal difference between the two series is the smaller step change in the carbonylation rate between methanol and the higher alcohols, compared with the oxidative addition reactions. This may be due to the different temperatures and the different reaction media used in the two sets of experiments. The activation parameters obtained for the oxidative addition reactions also resemble those for catalytic carbonylation; the increase in $\Delta H^{\ddagger}$ for higher alkyls compared with methyl is similar for both catalytic carbonylation and oxidative addition. Our data therefore support the conclusion that the oxidative addition step is key in the Rh/I$^-$ catalyzed carbonylation of alcohols. The somewhat anomalous results for ^{i}PrI may be related to Forster's observation of substantially larger rates for the carbonylation of 2-propanol, compared with *n*-propanol and ethanol. An electron transfer step in the oxidative addition mechanism may be at least partially responsible for these enhanced rates, but an alternate pathway involving hydrocarboxylation of propene is also likely for the more readily dehydrated secondary alcohol. Our results also provide direct evidence that the formation of isomeric carboxylic acids during carbonylation of *n*- or 2-propanol is due to alkyl isomerization at the metal center.

Conclusions

These results show that the reactions of $[M(CO)_2I_2]^-$ (M = Rh, Ir) with higher alkyl iodides, RI, giving $[Rh(CO)(COR)I_3]^-$ and $[RIr(CO)_2I_3]^-$, are analogous to those with methyl iodide, although much slower. Typi-

(25) Brumbaugh, J. S.; Sen, A. *J. Am. Chem. Soc.* **1988**, *110*, 803.

(26) (a) Bennett, M. A.; Charles, R.; Mitchell, T. R. B. *J. Am. Chem. Soc.* **1978**, *100*, 2737. (b) Bennett, M. A.; Jeffery, J. C. *Inorg. Chem.* **1980**, *19*, 3763. (c) Bennett, M. A.; Crisp, G. T. *Organometallics* **1986**, *5*, 1792. (d) Bennett, M. A.; Crisp, G. T. *Organometallics* **1986**, *5*, 1800.

cally, the relative rates for MeI and EtI are 1000:3, the higher iodides react somewhat slower still. The similarity to reactivity trends for organic nucleophiles suggests an S_N2 mechanism, but radical processes may also participate under some circumstances. Relative rates, k_{Ir}/k_{Rh} in the range 140–220, have been estimated for the two nucleophiles $[Rh(CO)_2I_2]^-$ and $[Ir(CO)_2I_2]^-$ for the three organic iodides compared.

Alkyl isomerization is observed for both $[Rh(CO)(COPr)I_3]^-$ and $[PrIr(CO)_2I_3]^-$, and in the rhodium system, reversible exchange with added alkene leads to interconversion of $[Rh(CO)(COPr)I_3]^-$ and $[Rh(CO)(COEt)I_3]^-$. A mechanism for these reactions involving hydrido–alkene intermediates is proposed.

Our model data support the conclusions of previous catalytic studies.[3] Both approaches indicate that the major route for catalytic carbonylation of linear primary alcohols proceeds via rate determining oxidative addition of RI to $[Rh(CO)_2I_2]^-$, analogous to the mechanism for methanol carbonylation. We have also shown that oxidative addition of ^{i}PrI is a feasible pathway in the carbonylation of isopropanol. However, in this case, an alternative route involving dehydration of the substrate alcohol and addition of olefin to a rhodium hydride probably plays an important role.

Experimental Section

Dichloromethane and acetonitrile were distilled from calcium hydride, nitromethane from calcium chloride, and diethyl ether from a purple solution of sodium/benzophenone under nitrogen, immediately prior to use. Propyl iodides were shaken with copper powder to remove traces of iodine, then distilled under reduced pressure to avoid decomposition, and stored in the dark over mercury. Ethyl iodide was dried with sodium wire and distilled.[27] All operations involving photosensitive alkyl iodides were protected from light with aluminum foil. Chloroform-d_3 and dichloromethane-d_2 for NMR measurements were distilled from molecular sieves (4 Å). Argon, nitrogen, and carbon monoxide were dried by molecular sieves (4 Å); carbon monoxide was also passed through a short column of activated charcoal to remove any iron pentacarbonyl impurity.[28] Standard Schlenk and cannula techniques were used for handling air and moisture sensitive materials.[29]

Solution IR spectra (CaF_2 cell, 0.2-mm path length) were measured on a Perkin-Elmer 1640 or Perkin-Elmer 1710 interferometer. ^{1}H and ^{13}C NMR spectra were recorded on Bruker AM250 or Bruker AC250 instruments. Microanalyses were determined by the University of Sheffield microanalysis service. GLC analyses were carried out on a Perkin-Elmer 8600 chromatograph fitted with a DB5 fused silica capillary column and an fid detector.

Synthesis of Complexes $(Ph_4As)_2[\{Rh(CO)(COR)I_3\}_2]$. $Ph_4As[Rh(CO)_2I_2]$ (0.3 g, 0.38 mmol)[2b] was dissolved in the appropriate neat alkyl iodide (dry, distilled, 10 mL) under nitrogen, and the solution was transferred to a stainless steel (Fisher–Porter) tube. The tube was heated to 80 °C in an oil bath under 5 atm of nitrogen (5 days). The tube was then allowed to cool to room temperature and the nitrogen pressure released. The dark red solution was filtered through Celite under nitrogen into a Schlenk tube. The solvent was removed under vacuum and the dark red oil recrystallized from dichloromethane and hexane at 0 °C. The solid product was found to be stable for 1 month if stored under nitrogen at 0 °C. The ^{1}H NMR spectra, recorded in $CDCl_3$, in each case showed multiplets at δ 7.80–7.90 and 7.63–7.68 (20H) corresponding to the tetraphenylarsonium cation. ^{1}H NMR data for the alkyl moieties of the anions **3b–c** are given in Table 1. Microanalytical data are given in Table 2; the anions are presumed dinuclear by analogy with $(Bu_4N)_2[\{Rh(CO)(COMe)I_3\}_2]$.[11]

$(Ph_4As)_2[\{Rh(CO)(COEt)I_3\}_2]$ (**3b**): yield 47%; ν(CO) 2062, 1768, and 1702 cm^{-1} (CH_2Cl_2).

$(Ph_4As)_2[\{Rh(CO)(CO^nPr)I_3\}_2]$ (**3c**): yield 47%; ν(CO) 2060 and 1750 cm^{-1} (CH_2Cl_2).

$(Ph_4As)_2[\{Rh(CO)I_3(CO^iPr)\}_2]$ (**3d**): yield 44%; ν(CO) 2060 and 1750 cm^{-1} (CH_2Cl_2).

Synthesis of $Ph_4As[Ir(CO)_2I_2]$. $Ph_4As[Ir(CO)_2I_2]$ was synthesized by a variation of the method described by Forster.[30] Carbon monoxide was passed through a refluxing solution of $IrCl_3{\cdot}3H_2O$ (0.3 g, 0.85 mmol) and NaI (2.5 g) dissolved in a mixture of 2-methoxyethanol (28.5 mL) and distilled water (1.5 mL), for 18 h. After addition of Ph_4AsCl (0.377 g, 0.9 mmol) dissolved in a minimum amount of 2-methoxyethanol (ca. 3 mL), the solution was filtered. Distilled water was added to the hot filtrate under carbon monoxide until precipitation occurred. The solution was allowed to cool to 0 °C under CO to give a crop of yellow crystals (yield 0.64 g, 85%), ν(CO) (CH_2Cl_2) 2046 and 1968 cm^{-1}.

Synthesis of Complexes $Ph_4As[RIr(CO)_2I_3]$. $Ph_4As[MeIr(CO)_2I_3]$ was prepared in high yield via the rapid reaction of $Ph_4As[Ir(CO)_2I_2]$ with neat methyl iodide at room temperature, as described by Forster.[14] The cognate complexes $Ph_4As[RIr(CO)_2I_3]$ were prepared in a similar manner. $Ph_4As[Ir(CO)_2I_2]$ (0.20 g, 0.23 mmol) was dissolved in CH_2Cl_2 (5 mL) in a foil wrapped Schlenk tube under a nitrogen atmosphere. The alkyl iodide (3 mL, large excess) was added and the reaction vessel placed in a water bath (30 °C, 16 h). After removal of the solvent and excess alkyl iodide in vacuo, the resultant yellow solid was washed with diethyl ether (2 × 10 mL) and dried in vacuo. The ^{1}H NMR spectra, recorded in $CDCl_3$, in each case showed multiplets at δ 7.80–7.90 and 7.63–7.68 (20H) corresponding to the tetraphenylarsonium cation. ^{1}H NMR data for the alkyl moieties of the anions **5a–g** are given in Table 1. Microanalytical data are given in Table 2.

$Ph_4As[EtIr(CO)_2I_3]$ (**5b**): yield 87%; ν(CO) 2094 and 2040 cm^{-1} (CH_2Cl_2); δ(^{13}C) ($CDCl_3$) 131.6, 133.0, 134.9 (Ph_4As), 155.6 (Ir–*C*O), 6.6 (Ir–*C*H$_2$), 26.9 (*C*H$_3$).

$Ph_4As[(^nPr)Ir(CO)_2I_3]$ (**5c**): yield 81%; ν(CO) 2094 and 2040 cm^{-1} (CH_2Cl_2); δ(^{13}C) ($CDCl_3$) 131.6, 133.0, 134.9 (Ph_4As), 155.6 (Ir–*C*O), 33.9 (Ir–CH$_2$–*C*H$_2$), 16.2 (Ir–*C*H$_2$), 18.3 (*C*H$_3$).

$Ph_4As[(^nBu)Ir(CO)_2I_3]$ (**5e**): yield 76%; ν(CO) 2094 and 2040 cm^{-1} (CH_2Cl_2).

$Ph_4As[(n\text{-}C_5H_{11})Ir(CO)_2I_3]$ (**5f**): yield 80%; ν(CO) 2094 and 2040 cm^{-1} (CH_2Cl_2).

$Ph_4As[(n\text{-}C_6H_{13})Ir(CO)_2I_3]$ (**5g**): yield 87%; ν(CO) 2094 and 2040 cm^{-1} (CH_2Cl_2).

The reaction of $Ph_4As[Ir(CO)_2I_2]$ with isopropyl iodide gave a mixture of $Ph_4As[(^iPr)Ir(CO)_2I_3]$ (ν(CO) 2094 and 2040 cm^{-1}, CH_2Cl_2) and $Ph_4As[Ir(CO)_2I_4]$ (ν(CO) 2112 and 2068 cm^{-1}, CH_2Cl_2) (ca. 75:25 ratio by IR).

X-ray crystal Data for $Ph_4As[(n\text{-}C_6H_{13})Ir(CO)_2I_3]$ (5g): $C_{32}H_{33}AsI_3IrO_2$; M = 1097.47; crystallized from dichloromethane/diethyl ether as red/orange blocks; crystal dimensions 0.80 × 0.4 × 0.4 mm;[31] monoclinic, a = 9.408(7) Å, b = 19.470(16) Å, c = 19.529(12) Å, β = 94.99(5)°, V = 3564(4) Å^3, Z = 4, D_c = 2.045 g cm^{-3}, space group $P2_1/n$ (a nonstandard setting of $P2_1/c$

(27) Hammond, G. S.; Hawthorne, M. F.; Waters, J. H.; Graybill, D. M. *J. Am. Chem. Soc.* **1960**, *82*, 704.

(28) Haynes, A.; Ellis, P. R.; Byers, P. K.; Maitlis, P. M. *Chem. Br.* **1992**, *28*, 517.

(29) (a) Shriver, D. F. *The Manipulation of Air Sensitive Compounds*, 2nd ed.; Wiley: New York, 1986. (b) *Experimental Organometallic Chemistry*; Wayda, A. L., Darensbourg, M. Y., Eds.; ACS Symposium Series No. 357; American Chemical Society: Washington, DC, 1987; Chapter 2.

(30) Forster, D. *Inorg. Nucl. Chem. Lett.* **1969**, *5*, 433.

(31) Even these crystals were very fragile and attempts to cut them down to a smaller size were quite unsuccessful and resulted in complete disintegration.

C_{2h}^5, No. 14), Mo Kα radiation ($\bar{\lambda}$ = 0.710 69 Å), μ(Mo Kα) = 72.49 cm^{-1}, F(000) = 2039.63.

Three-dimensional, room temperature X-ray data were collected in the range 3.5 < 2θ < 45° on a Nicolet R3 diffractometer by the ω-scan method. The 2446 independent reflections (of 5197 measured) for which $|F|/\sigma(|F|) > 4.0$ were corrected for Lorentz and polarization effects and for absorption by Gaussian integration methods (minimum and maximum transmission coefficients 0.030 and 0.097). The structure was solved by direct methods and refined by blocked cascade least squares methods. Tight geometric constraints were applied to both carbonyls, to the hexyl chain, and to the four phenyl rings. The high thermal parameters of the alkyl carbons in particular suggested some disorder which resisted a more structural modeling. Hydrogen atoms were included in calculated positions and refined in the riding mode. Refinement converged at a final R = 0.0966 (R_w = 0.0921, 238 parameters, mean and maximum δ/σ 0.008, 0.041), with allowance for the thermal anisotropy of iridium, iodine, arsenic, and 22 carbon atoms. The minimum and maximum final electron densities were −1.86 and +1.82 e Å^{-3}. A weighting scheme $w^{-1} = \sigma^2(F) + 0.00100(F)^2$ was used in the latter stages of refinement. Complex scattering factors were taken from ref 32 and from the program package SHELXTL[33] as implemented on the Data General DG30 computer. The anisotropic thermal vibration parameters and H position parameters (with estimated standard deviations) are given in the supplementary material.

Kinetics of the Reaction of Alkyl Iodides with $Ph_4As[Rh(CO)_2I_2]$. An empty stainless steel (Fisher−Porter) tube (capacity ca. 50 mL) was connected to the gas handling manifold and the Heidolph EKT 3000 contact thermometer set to the required temperature. The oil bath was preheated to prevent an initial drop in oil bath temperature on immersion of a cold reaction vessel. When the reaction temperature was reached, the tube was disconnected and a weighed quantity of $Ph_4As[Rh(CO)_2I_2]$ (ca. 50 mg), alkyl iodide (8 mL), and a magnetic stirrer bar were placed into the tube. The tube was quickly reconnected to the manifold and pressurized with 5 atm of nitrogen and then vented and repressurized to flush out remaining air. The oil bath was raised until the tube was half immersed in the oil bath, and the stopwatch was started. At regular intervals, the tube was removed from the oil bath and the pressure released. A small portion of the reaction mixture was removed by pipette and cooled in a small sample tube immersed in ice. The steel tube was quickly reconnected to the rig and 5 atm of nitrogen introduced. An infrared spectrum of the reaction sample was then recorded and stored for subsequent extraction of absorbance intensities for kinetic analysis.

Kinetics of the Reactions of Alkyl Iodides with $Ph_4As[Ir(CO)_2I_2]$. Kinetics were measured under pseudo-first-order conditions (a large excess of RI to iridium complex), by monitoring both the decay of the low frequency ν(CO) of $[Ir(CO)_2I_2]^-$ at 1963 cm^{-1} and the growth of the high frequency band of the product, $[RIr(CO)_2I_3]^-$ at 2089 cm^{-1} (ν(CO) in neat RI solvent). In a typical kinetic experiment, the alkyl iodide (2.5 mL) was transferred by syringe into a 5-mL graduated flask containing an accurately weighed amount of duroquinone (ca. 2−3 mg) if so required. The flask was then filled with the appropriate solvent, stoppered with a suba seal and shaken to ensure complete dissolution of the duroquinone. A small portion of the solution was removed by syringe under argon and used to record the background solvent spectrum. $Ph_4As[Ir(CO)_2I_2]$ (30 mg, 3.4 × 10^{-5} mol) was accurately weighed into a 5-mL graduated flask which was evacuated before argon was introduced. The alkyl iodide solution was then added by syringe and the flask stoppered and shaken to ensure homogeneity. An aliquot was transferred by syringe into the thermostated IR cell (CaF_2, 0.5-mm path length) which had been thoroughly flushed with argon. The measurement of spectra at regular intervals was automated using the Obey programming language on a PE3600 data station attached to the PE1710 spectrometer. Rate constants obtained using the above procedure were reproducible to within ±6%. The values reported are averages of the runs performed.

Acknowledgment. We thank the SERC and BP Chemicals Ltd. for CASE awards (to P.R.E., J.M.P.), BP Chemicals Ltd. for generous financial support (to A.H.), Drs. Glenn Sunley, Carl Garland, and George Morris for helpful discussions, and the University of Sheffield for assistance with the provision of equipment.

Supplementary Material Available: Tables of bond lengths and angles, thermal parameters, H coordinates, and kinetic data and Eyring plots (7 pages). Ordering information is given on any current masthead page.

OM9402269

(32) *International Tables for X-ray crystallography*; Kynoch Press: Birmingham, U.K., 1974; Vol. 4.

(33) Sheldrick, G. M. SHELXTL, An Integrated System for Solving, Refining and Displaying Crystal Structures from Diffraction Data (Revision 5.1). University of Gottingen, Germany, 1985.